Z. Phys. C - Particles and Fields 29, 423–437 (1985)

Zeitschrift für Physik C Particles and Fields

Single Hadron Spectrum in $\gamma\gamma$ Collisions: The QCD Contribution to Order α_S and the Non Perturbative Background

P. Aurenche, A. Douiri[1]
LAPP, F-74019 Annecy-le-Vieux, France

R. Baier
Fakultät für Physik, Universität Bielefeld, D-4800 Bielefeld 1, Federal Republic of Germany

M. Fontannaz, D. Schiff
Laboratoire de Physique Théorique et Hautes Energies,[2] Bât. 211, Université Paris-Sud, F-91405 Orsay, France

Received 13 June 1985

Abstract. We calculate the corrections of order α_S to the process $\gamma\gamma \to HX$ where both initial photons are real. The analytic expressions are given and a detailed discussion of the variation of the corrections with p_T and rapidity is presented. The dependence on the factorization prescription and scale is also discussed. Using the equivalent photon approximation the cross-section for $e^+e^- \to e^+e^- HX$ is calculated both in the PEP/PETRA and LEP energy range. Based on the vector meson dominance model the non perturbative background is estimated and its importance for present and future experiments is emphasized.

The photon–photon reactions represent an important class of scattering processes which allow for fundamental tests of Quantum Chromodynamics. Besides their specific relevance for the production of resonances of even C-parity, they can provide important constraints on the validity of the standard model of Strong Interactions through the study of inclusive hadron production [1]. Indeed, except for the fragmentation functions describing the hadronization of final state partons, the single particle spectrum at large p_T is completely calculable from perturbative QCD. In the parton model, this cross-section is proportional to Σe_q^4, e_q denoting the quark charges. On the basis of this quantity, models with integrally charged quarks and fractionally charged quarks can in principle be distinguished. In fact, two other classes of reactions, the deep inelastic Compton effect $\gamma p \to \gamma X$ and the production of two photons in hadronic collisions $HH' \to \gamma\gamma X$, which are related to $\gamma\gamma \to HX$ via crossing symmetry at the partonic level, involve the same factor Σe_q^4. As recently reported [2], it seems that models with integer charge (even in their broken color symmetry version [3]) have difficulties in the photon photoproduction data as well as in γ–γ correlations in hadronic collisions with the same choice of parameters as those derived from γ–γ collisions [2].

Concerning the standard model of Strong Interactions, a quantitative comparison with the data is reliable only when the higher order corrections have been taken into account. Such a calculation has been performed for the deep inelastic Compton process [4, 5] and very good agreement is obtained with the recent NA14 data [6]. On the other hand, a partial calculation of higher order effects [7, 8] to the reaction $\gamma\gamma \to HX$ has led to small corrections which cannot account for the discrepancy between the preliminary PETRA data [9–11] and the lowest order estimates. We report here on a more complete calculation. It is part of a systematic study of all processes [5, 12, 13] involving one or two real photons in the initial and/or final state. The consideration of all these processes together imposes a most stringent set of constraints on perturbative QCD as well as on the shape of the structure functions involved.

Higher order corrections to $\gamma\gamma$ collisions had already been considered by Berends, Gastmans and Kunszt [14] for the production of jets. In contrast we make predictions for single particle inclusive cross-sections which avoid the ambiguity of the theoretical and experimental definitions of jets. In our case, the comparison with data is more straightforward. Compared to the work of Khalafi, Landshoff and Stirling

1 On leave of absence from LMPHE, Faculté des Sciences, Rabat, Maroc
2 Laboratoire associé au CNRS

[7, 8] ours is more general: i) we take into account the contribution of the gluon fragmentation to the single hadron spectrum and we do not restrict the calculation to the production of particles at zero rapidity in the $\gamma\gamma$ center of mass*; ii) out results are also presented with the initial photon energy spectrum folded in to make comparison with experimental results for untagged $e^+e^- \to e^+e^- HX$ meaningful.

We shall first briefly recall the lowest order results in order to define the notation. In the second and third sections we turn to the evaluation of the $\mathcal{O}(\alpha_S)$ diagrams: they lead to two classes of terms: the genuine higher order corrections and the leading order corrections associated to the anomalous photon component. A detailed discussion is then given for an energy typical of the PETRA/PEP energy range: the rôle of the choice of factorization scales and prescription is analysed. Using the equivalent photon approximation, we present in a last section the results for $e^+e^- \to e^+e^- HX$ with untagged leptons. A careful discussion and evaluation of the vector dominance contribution is also given and its importance at present energies is stressed. Finally we give predictions for the LEP energy range.

I. The Lowest Order Results

In perturbative QCD, the relationship between hadronic and partonic cross-sections is given by the general formula

$$E\frac{d^3\sigma}{d^3P} = \sum_{i,j,f} \int dx_1 dx_2 F_{i,1}(x_1) F_{j,2}(x_2) \cdot \frac{dx}{x^2} D_{f,H}(x) p^\circ \frac{d\hat{\sigma}^{ij\to f}}{d^3p} \tag{1}$$

where x_1 (resp. x_2) is the fraction of momentum of the interacting parton i (resp. j) in the initial hadron 1 (resp. 2) and x is the fraction of momentum carried by the observed hadron H decaying from the final state parton f. The symbol $\hat{\sigma}^{ij\to f}$ denotes the partonic cross-section evaluated at a given order of perturbation theory. The structure functions of type $F_{i,1}(x_1)$ and the decay probability $D_{f,H}(x)$ have no scaling violations. Neglecting, for the moment, the hadronic component of the photon (VDM) the functions $F_{i,1}(x_1)(F_{j,2}(x_2))$ are δ-functions and $p^0(d^3\hat{\sigma}^{ij\to f}/d^3p)$ describes the process $\gamma\gamma \to q\bar{q}$ at the lowest order (Fig. 1). The aim of this paper being the computation of higher order QCD corrections we shall present the lowest order result in a way useful for later discussion. The calculation of inclusive cross-sections to higher orders involves divergencies. These divergencies are isolated using the dimensional regularization [15] method which requires working in a space of $n = 4 - 2\varepsilon$ dimensions: the partonic cross-section becomes

* Where the two calculations overlap they are in agreement except for a minor difference: in (2.12) of [17], the term (-7) should be replaced by (-6). This is numerically insignificant

Fig. 1. The lowest order (Born) diagrams in photon–photon collisions

$$p^\circ \frac{d^3\hat{\sigma}^{\gamma\gamma\to q\bar{q}}}{d^3p} = \frac{1}{\Gamma(1-\varepsilon)}\left(\frac{4\pi\hat{s}}{\hat{t}\hat{u}}\right)^\varepsilon \frac{1}{(4\pi)^2}\frac{1}{\hat{s}} \cdot \delta(\hat{s}+\hat{t}+\hat{u})\bar{\Sigma}|\mathcal{M}|^2 \tag{2}$$

where the properly summed and averaged matrix element squared is given by (see Fig. 1 for notation)

$$\bar{\Sigma}|\mathcal{M}|^2 = 2N_C(4\pi\alpha)^2 e_q^4 \mu^{4\varepsilon}(1-\varepsilon) \cdot \left((1-\varepsilon)\left(\frac{\hat{t}}{\hat{u}}+\frac{\hat{u}}{\hat{t}}\right) - 2\varepsilon\right) \tag{3}$$

In this expression, as well as in the rest of this paper, all fields are chosen to be massless. The arbitrary mass scale μ is introduced to keep the action dimensionless when working in an n-dimensional space. N_C is the number of colors.

For γ–γ collisions the relationship between partonic and external kinematics (labelled with capital letters) is very simple. One has

$$\hat{s} = S, \quad \hat{t} = T/x, \quad \hat{u} = U/x, \quad p_T^2 = UT/S. \tag{4}$$

It is useful to introduces the scaled variables [17]

$$1 - V = -T/S, \quad W = -U/(T+S)$$
$$Z = 1 - V + VW \quad 1 - v = -\hat{t}/\hat{s},$$
$$w = -\hat{u}/(\hat{t}+\hat{s}) \tag{5}$$

with the relations

$$v = 1 - \frac{1-V}{x}, \quad w = \frac{VW}{vx}. \tag{6}$$

Equation (2) is then conveniently written after a change of variables,

$$p^\circ \frac{d^3\sigma^{\gamma\gamma\to q\bar{q}}}{d^3p} = \frac{1}{\pi\hat{s}}\frac{1}{v}\frac{d\hat{\sigma}^{\gamma\gamma\to q\bar{q}}}{dv}(\hat{s}, v)\delta(1-w) \tag{7}$$

with

$$\frac{d\hat{\sigma}^{\gamma\gamma\to q\bar{q}}}{dv}(\hat{s}, v) = \frac{1}{\Gamma(1-\varepsilon)}\left(\frac{4\pi}{\hat{s}v(1-v)}\right)^\varepsilon \frac{1}{16\pi}\bar{\Sigma}\frac{|\mathcal{M}|^2}{\hat{s}} \tag{8}$$

For the numerical evaluation of the physical cross-section, the limit $\varepsilon = 0$ is taken and

$$E\frac{d^3\sigma}{d^3P} = \sum_{i=q,\bar{q}} \int_Z^1 \frac{dx}{x^2} D_{i,H}(x) \frac{1}{\pi S}\frac{1}{v} \cdot \frac{d\hat{\sigma}^{\gamma\gamma\to q\bar{q}}}{dv}(\hat{s}, v)\delta(1-w). \tag{9}$$

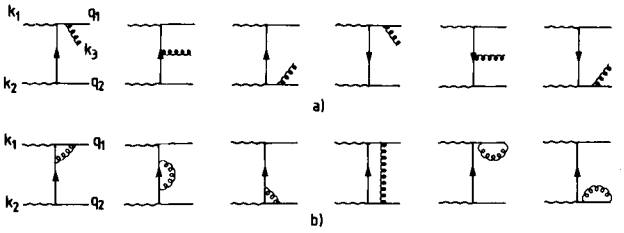

Fig. 2 a and b. Diagrams of order α_S contributing to photon–photon collisions. **a** Real diagrams. **b** Virtual diagrams. (A similar set with k_1 and k_2 interchanged is not shown)

II. The Perturbative Calculation

The higher order corrections considered in this work are those arising from the diagrams shown in Fig. 2, obtained by coupling a gluon to the lowest order terms. The properly averaged matrix element squared for the diagrams of Fig. 2a can be obtained by crossing from the corresponding ones appearing in the deep inelastic Compton scattering [5]. The result is

$$\begin{aligned}\tfrac{1}{4}\Sigma|\mathcal{M}|^2 = {} & (4\pi)^3\alpha^2 e_q^4\alpha_S(\mu)C_F N_C\mu^{6\varepsilon}\\ & \cdot 2q_1\cdot q_2\\ & \cdot q_1\cdot k_1 q_1\cdot k_2 q_1\cdot k_3 q_2\cdot k_1 q_2\cdot k_2 q_2\cdot k_3\\ & \cdot\{(1-\varepsilon)^2[q_1\cdot k_1 q_2\cdot k_1((q_1\cdot k_1)^2+(q_2\cdot k_1)^2)\\ & +(k_1\to k_2)+(k_1\to k_3)]\\ & -\varepsilon(1-\varepsilon)[q_1\cdot k_1 q_2\cdot k_1(q_1\cdot k_2\\ & -q_2\cdot k_2)(q_1\cdot k_3-q_2\cdot k_3)\\ & +(k_1\leftrightarrow k_2)-(k_1\leftrightarrow k_3)]\\ & +\varepsilon(2+\varepsilon)[(q_1\cdot k_1 q_2\cdot k_1)^2+(k_1\to k_2)\\ & +(k_1\to k_3)]\\ & -2\varepsilon(4-\varepsilon)[q_1\cdot k_1 q_2\cdot k_1 q_1\cdot k_2 q_2\cdot k_2\\ & +(k_1\to k_3)+(k_2\to k_3)]\}. \end{aligned}\tag{10}$$

When calculating the differential partonic cross-section appearing in (1) one keeps fixed the momentum of parton f [f can be a quark, an antiquark or a gluon] which emits the observed hadron and performs analytically the phase space integration over the other partons. Divergencies associated with collinear configurations appear as poles in ε: these singular pieces have a simple interpretation and can be written as convolutions of Altarelli–Parisi splitting functions with $2\to 2$ cross-sections [16]. In the case where the observed hadron is emitted by the quark or the antiquark, infrared singularities also appear when the gluon momentum vanishes: they are cancelled by terms arising from the interference of virtual diagrams of Fig. 2b with the Born terms which contribute to the same kinematical configuration. These virtual terms can be calculated using the techniques of [15]. The result, in the Feynman gauge, is

$$\begin{aligned}\frac{d\hat\sigma}{dv}(\hat s,v)\Big|_{\text{virtual}} = {} & \frac{\alpha_S(\mu)}{2\pi}\frac{1}{\Gamma(1-2\varepsilon)}\left(\frac{4\pi\mu^2}{\hat s}\right)^{\varepsilon}\\ & \cdot\left(\frac{4\pi\mu^2}{\hat s v(1-v)}\right)^{\varepsilon}\mu^{2\varepsilon}\frac{2\pi\alpha^2 e_q^4}{\hat s}C_F N_C\\ & \cdot\left[\left(-\frac{2}{\varepsilon^2}+\frac{1}{\varepsilon}\right)\left(\frac{v}{1-v}+\frac{1-v}{v}\right)+\frac{4}{\varepsilon}\right]\\ & +\frac{\alpha_S(\mu)}{2\pi}\frac{2\pi\alpha^2 e_q^4}{\hat s}C_F N_C\\ & \cdot\left[\left(\frac{2\pi^2}{3}-3+\ln^2 v+\ln^2(1-v)\right)\right.\\ & \cdot\left(\frac{v}{1-v}+\frac{1-v}{v}\right)+2\\ & +\left(2+3\frac{1-v}{v}\right)\ln v\\ & +\left(2+\frac{3v}{1-v}\right)\ln(1-v)\\ & +\left(2+\frac{v}{1-v}\right)\ln^2 v\\ & \left.+\left(2+\frac{1-v}{v}\right)\ln^2(1-v)\right]. \end{aligned}\tag{11}$$

The method of phase space integration in n-dimensions for the case of three particles in the final state [17–20] is, by now, fairly standard and it can be applied to (10) to obtain the first order perturbative result for the process $\gamma\gamma\to q\bar q g$ which can be expressed (for one flavor) as:

$$\begin{aligned}E\frac{d^3\sigma}{d^3P} = {} & \int_Z^1\frac{dx}{x^2}D_{q,H}(x)\left[\frac{1}{\pi S}\frac{1}{v}\frac{d\hat\sigma^{\gamma\gamma\to q\bar q}}{dv}(S,v)\delta(1-w)\right.\\ & +\frac{\alpha_S}{2\pi}H_{qq}\left(\frac{Z}{x},\varepsilon,Q^2\right)\frac{1}{\pi S}\frac{x}{Z}\frac{d\hat\sigma^{\gamma\gamma\to q\bar q}}{dv}\left(S,\frac{xvw}{Z}\right)\\ & +\frac{\alpha}{2\pi}\left(H_{q\gamma}(w,\varepsilon,Q^2)\frac{1}{\pi S}\frac{1}{v}\frac{d\hat\sigma^{\gamma q\to gq}}{dv}(wS,v)\right.\\ & +H_{q\gamma}\left(\frac{1-v}{1-vw},\varepsilon,Q^2\right)\frac{1}{\pi S}\frac{1}{1-vw}\frac{d\hat\sigma^{\gamma q\to gq}}{dv}\\ & \left.\left.\cdot\left(\frac{1-v}{1-vw}S,1-vw\right)\right)+\frac{\alpha_S}{2\pi}k_q(v,w,Q^2,S)\right]\\ & +\int_Z^1\frac{dx}{x^2}D_{g,H}(x)\left[\frac{\alpha_S}{2\pi}H_{gq}\left(\frac{Z}{x},\varepsilon,Q^2\right)\frac{1}{\pi S}\frac{x}{Z}\right.\\ & \cdot\frac{d\hat\sigma^{\gamma\gamma\to q\bar q}}{dv}\left(S,\frac{vwx}{Z}\right)+\frac{\alpha_S}{2\pi}k_g(v,w,Q^2,S)\\ & +\frac{\alpha}{2\pi}\left(H_{q\gamma}(w,\varepsilon,Q^2)\frac{1}{\pi S}\frac{1}{v}\frac{d\hat\sigma^{\gamma q\to gq}}{dv}(wS,1-v)\right.\\ & +H_{q\gamma}\left(\frac{1-v}{1-vw},\varepsilon,Q^2\right)\frac{1}{\pi S}\frac{1}{1-vw}\frac{d\hat\sigma^{\gamma q\to gq}}{dv}\\ & \left.\left.\left.\cdot\left(\frac{1-v}{1-vw}S,vw\right)\right)\right)\right]. \end{aligned}\tag{12}$$

In the above expression the singular terms associated to mass singularities are separated off. Those which are proportional to H_{qq} or H_{gq} correspond to the collinear fragmentation of the final state parton $q \to q$ or $q \to g$ and they contain the Altarelli-Parisi splitting functions

$$H_{iq}(x,\varepsilon,Q^2) = \left(-\frac{1}{\varepsilon}\right)\frac{\Gamma(1-\varepsilon)}{\Gamma(1-2\varepsilon)}\left(\frac{4\pi\mu^2}{Q^2}\right)^{\varepsilon} P_{iq}(x) \tag{13}$$

with

$$P_{gq}(x) = C_F\left(\frac{1+x^2}{(1-x)_+} + \tfrac{3}{2}\delta(1-x)\right),$$
$$P_{gq} = C_F\frac{1+(1-x)^2}{x} \tag{14}$$

(the symbol $(g(x))_+$ denotes, as usual, the prescription $\int_0^1 (g(x))_+ f(x)dx = \int_0^1 (f(x)-f(1))g(x)dx$). The function $H_{q\gamma}$ describes the collinear fragmentation of a photon into a quark-antiquark pair and it takes the form

$$H_{q\gamma}(x,\varepsilon,Q^2) = e_q^2\left(-\frac{1}{\varepsilon}\right)\frac{\Gamma(1-\varepsilon)}{\Gamma(1-2\varepsilon)}\left(\frac{4\pi\mu^2}{Q^2}\right)^{\varepsilon} \cdot N_C(x^2+(1-x)^2) \tag{15}$$

while the differential cross-section for the process $\gamma q \to gq$ is given by

$$\frac{1}{\pi}\frac{d\hat{\sigma}^{\gamma q\to gq}}{dv}(S,v) = \frac{\mu^{2\varepsilon}}{\Gamma(1-\varepsilon)}\left(\frac{4\pi\mu^2}{Sv(1-v)}\right)^{\varepsilon}\alpha e_q^2\alpha_S\frac{2C_F}{S} \cdot(1-\varepsilon)\left((1-\varepsilon)\left(v+\frac{1}{v}\right)+2\varepsilon\right). \tag{16}$$

The mass scale Q appearing in the singular functions H_{ij} depends on the external variables but is otherwise arbitrary. We shall discuss later on specific expressions for Q^2. Finally the functions $k_q(v,w,Q^2,S)$ and $k_g(v,w,Q^2,S)$ are finite in the limit $\varepsilon \to 0$, as a consequence of the factorization theorem [16] at order α_S.

III. Definition of the Corrections

The divergent pieces appearing in the perturbative calculation are, as usual, eliminated, with the help of the factorization theorem, by the introduction of scale violating structure and fragmentation functions. Consider first the contribution to $Ed^3\sigma/d^3P$ of all terms proportional to $d\hat{\sigma}^{\gamma\gamma\to q\bar{q}}/dv$ in (12). They can be written as

$$\frac{1}{\pi SZ}\frac{d\hat{\sigma}^{\gamma\gamma\to q\bar{q}}}{dv}\left(S,\frac{VW}{Z}\right)\left[D_{q,H}(Z) + \frac{\alpha_S}{2\pi}\int_Z^1\frac{dx}{x}\left(D_{q,H}(x)H_{qq}\left(\frac{Z}{x},\varepsilon,Q^2\right) + D_{g,H}(x)H_{gq}\left(\frac{Z}{x},\varepsilon,Q^2\right)\right)\right]. \tag{17}$$

The expression in square brackets defines the scaling violating quark fragmentation function:

$$D_{q,H}(Z,Q^2) = D_{q,H}(Z) + \frac{\alpha_S}{2\pi}\int_Z^1\frac{dx}{x}\left(D_{q,H}(x)H_{qq}\left(\frac{Z}{x},\varepsilon,Q^2\right) + D_{g,H}(x)H_{gq}\left(\frac{Z}{x},\varepsilon,Q^2\right)\right). \tag{18}$$

This definition introduces the so-called universal fragmentation function since the relationship between the bare quantity $D_{i,H}(x)$ and the scaling violating one is independent of the process considered (the functions P_{qq} and P_{gq} are universal). Another, more practical definition, which is process dependent, relates the scaling violating quantity directly to the cross-section for the inclusive reaction $e^+e^- \to HX$ [21, 22] in the photon approximation. More precisely, following [22] one writes

$$\frac{\sigma_T^H(Z,Q^2)}{3\sigma_0} = \sum_{i=q,\bar{q}} e_q^2 \bar{D}_{i,H}(Z,Q^2) \tag{19}$$

where σ_T^H is the inclusive cross-section, for transversely polarized virtual photons, and $\sigma_0 = 4\pi\alpha^2/(3Q^2)$ is the cross-section for the process $e^+e^- \to \mu^+\mu^-$. The relationship between the two choices is simply given by

$$\bar{D}_{q,H}(Z,Q^2) = D_{q,H}(Z,Q^2) + \int_Z^1\frac{dx}{x}\frac{\alpha_S}{2\pi}\left(D_{q,H}\left(\frac{Z}{x},Q^2\right)d_{qq}(x) + D_{g,H}\left(\frac{Z}{x},Q^2\right)d_{gq}(x)\right) \tag{20}$$

with*

$$d_{qq}(x) = C_F\left((1+x^2)\left(\frac{\ln(1-x)}{1-x}\right)_+ + 2\frac{1+x^2}{1-x}\ln x + \frac{3}{2}\left(1-x-\left(\frac{1}{1-x}\right)_+\right) + \left(\frac{2\pi^2}{3}-\frac{9}{2}\right)\delta(x-1)\right)$$
$$d_{gq}(x) = C_F\left(\frac{1+(1-x)^2}{x}(\ln(1-x)+2\ln x) - 2\frac{1-x}{x}\right). \tag{21}$$

* Another definition proposed in [21] is

$$\sigma^H(Z,Q^2) = 3\sigma^0\left(1+\frac{\alpha_S}{\pi}\right)\sum_{i=q,\bar{q}} e_i^2 D_{i,H}(Z,Q^2)$$

which implies the changes [22]

$$d_{qq}(x) \to d_{qq}(x) + C_F(1-\tfrac{3}{2}\delta(x-1))$$
$$d_{gq}(x) \to d_{gq}(x) + C_F\frac{2(1-x)}{x}$$

The remaining divergent pieces in (12) are dealt with along similar lines. The photon structure function is introduced via the following procedure: we isolate in (12) the quantity:

$$F^{(0)}_{q,\gamma}(x,Q^2)=\frac{\alpha}{2\pi}H_{q\gamma}(x,\varepsilon,Q^2)+\frac{\alpha}{2\pi}f_{q\gamma}(x) \tag{22}$$

which is the result of the naive quark–parton model (QPM) for the quark distribution inside the photon [23], related to the photon structure function in $\gamma^*\gamma$ deep inelastic collisions by:

$$F_{2,\gamma}(x,Q^2)=2x\sum_{i=q,\bar{q}}e_i^2F^{(0)}_{i,\gamma}(x,Q^2). \tag{23}$$

The expression for $f_{q\gamma}(x)$ is [24]*:

$$f_{q\gamma}(x)=e_q^2N_C\left((x^2+(1-x)^2)\ln\frac{1-x}{x}+6x(1-x)\right) \tag{24}$$

The singularity contained in (22) is no longer present in the result of the QCD analysis which modifies the QPM answer by taking into account gluon emission [25]: evolution equations are written which allow to define $F_{q,\gamma}(x,Q^2)$, the expression of which reduces for very large Q^2 to the asymptotic "anomalous component" proportional to $\ln Q^2/\Lambda^2$. The function $F_{q,\gamma}(x,Q^2)$ (which should be compared to the measured photon structure function) is then used in (12) instead of $F^{(0)}_{q,\gamma}(x,Q^2)$. We shall come back in the next section to the detailed expressions which may be used.

When (12) is rewritten in terms of the scaling violating structure functions introduced in (19) and (23), the perturbative expression of the cross-section for the process $\gamma\gamma\to HX$, including the diagrams of Fig. 2, can be decomposed into

$$E\frac{d^3\sigma^{\mathrm{BORN}}}{d^3P}=\alpha^2\sum_{i=q,\bar{q}}e_i^4\bar{D}_{i,H}(Z,Q^2)\frac{2N_C}{S^2Z}\left(\frac{1-V}{VW}+\frac{VW}{1-V}\right) \tag{25}$$

$$E\frac{d^3\sigma^{\mathrm{ANOM}}}{d^3P}=\frac{2\alpha C_F}{S^2}\sum_{i=q,\bar{q}}e_i^2\int_Z^1\frac{dx}{x}\left\{\frac{F_{i,\gamma}(w,Q^2)}{VW}\alpha_S(Q^2)\left[\bar{D}_{i,H}(x,Q^2)\left(v+\frac{1}{v}\right)+D_{g,H}(x,Q^2)\left(1-v+\frac{1}{1-v}\right)\right]\right.$$
$$\left.+\frac{F_{i,\gamma}\left(\frac{1-v}{1-vw},Q^2\right)}{1-V}\alpha_S(Q^2)\left[\bar{D}_{i,H}(x,Q^2)\left(1-vw+\frac{1}{1-vw}\right)+D_{g,H}(x,Q^2)\left(vw+\frac{1}{vw}\right)\right]\right\} \tag{26}$$

$$E\frac{d^3\sigma^{HO}}{d^3P}=\int_Z^1\frac{dx}{x^2}\frac{\alpha_S(Q^2)}{2\pi}\left(\sum_{i=q,\bar{q}}\bar{D}_{i,H}(x,Q^2)K_i(v,w,Q^2,S)+D_{g,H}(x,Q^2)K_g(v,w,Q^2,S)\right) \tag{27}$$

with

$$K_i(v,w,Q^2,S)=k_i(v,w,Q^2,S)-\frac{\alpha^2e_i^4}{S^2}2\left\{C_F\left[\frac{f_{q\gamma}(w)}{vw}\left(v+\frac{1}{v}\right)+\frac{f_{q\gamma}\left(\frac{1-v}{1-vw}\right)}{1-v}\left(1-vw+\frac{1}{1-vw}\right)\right]\right.$$
$$\left.+N_C\frac{d_{qq}(1-v+vw)}{1-v+vw}\left(\frac{1-V}{VW}+\frac{VW}{1-V}\right)\right\}$$

$$K_g(v,w,Q^2,S)=k_g(v,w,Q^2,S)-\sum_{i=q,\bar{q}}\frac{\alpha^2e_i^4}{S^2}2\left\{C_F\left[\frac{f_{q\gamma}(w)}{vw}\left(1-v+\frac{1}{1-v}\right)+\frac{f_{q\gamma}\left(\frac{1-v}{1-vw}\right)}{1-v}\left(vw+\frac{1}{vw}\right)\right]\right.$$
$$\left.+N_C\frac{d_{qq}(1-v+vw)}{1-v+vw}\left(\frac{1-V}{VW}+\frac{VW}{1-V}\right)\right\}. \tag{28}$$

* One also finds in the literature a different expression for $f_{q\gamma}(x)$ where the term $6x(1-x)$ is replaced by $8x(1-x)-1$. This comes from a different convention when performing the photon spin summation in n-dimensions. The physical results are independent on the choice of the convention, provided the same choice is made when relating different processes through the factorization theorem

In this expression, the functions $f_{q\gamma}$ (resp. d_{qq} and d_{gq}) must be set equal to zero if the anomalous photon component in (26) (resp. the quark fragmentation function) is defined in the universal convention. To the order $\alpha_S(\mu)$ at which we do the calculation, only the quark fragmentation function is unambiguously defined. To resolve the ambiguity of the gluon fragmentation function would require performing the perturbative calculation to order α_S^2. Likewise, the choice of $\mu^2 = Q^2$ as the scale in the strong coupling constant is arbitrary since the correction itself is of first order in α_S. It should be emphasized that in (28), the functions k_q and k_g result from the direct perturbative calculation of the process $\gamma\gamma \to qqg$ while the other terms are related to the factorization prescription. It will be seen, in the next section, that such terms play an important rôle in the structure of the correction. The expressions for K_q and K_g are reported in Appendix B.

IV. Discussion of the Results

We have just seen that the calculation of the higher order diagrams leads to two types of corrections beyond the Born term: the genuine higher order corrections and the terms proportional to the photon structure function. It has been stressed recently [26] that the full non asymptotic QCD result should be used in the theoretical expression for $F_{q,\gamma}(x, Q^2)$. This implies a non perturbative input which may be taken from experiment. Actually, present experimental data for $\gamma^*\gamma$ deep inelastic scattering do not allow a refined analysis and one may use the naive picture which describes the photon structure function as a superposition of two components [11]: the anomalous component written in the leading logarithmic approximation [25] (or with equivalent agreement to the data, in the QPM approximation: $F_{q,\gamma}(x) = \alpha/2\pi e_q^2 N_C(x^2 + (1-x)^2) \ln (Q^2/\Lambda^2)$ and the hadronic component estimated in the VDM model. Therefore, the expression for $F_{q,\gamma}(x, Q^2)$ in (26) will be written according to such a simple description.

The anomalous photon structure function contains a factor $1/\alpha_S(Q^2)$ which cancels against the $\alpha_S(Q^2)$ coupling associated with the cross-section $\gamma q \to gq$ so that its contribution in (26) is of the same order as the Born term. At the order α_S level at which we carried out the calculation only one of the two photons may scatter through its quark constituent. Consideration of diagrams of order α_S^2 would imply the presence of the gluon component of the photon, leading to the processes of Fig. 3b which contribute, for the reason given above, to the same order as the Born term. The relevant expression to added to (26) is then

$$E\frac{d^3\sigma^{\mathrm{ANOM}}}{d^3P} = \frac{\alpha}{S^2}\sum_{i=q,\bar{q}} e_i^2 \int_z^1 \frac{dx}{x} D_{i,H}(x, Q^2)\alpha_S(Q^2) \cdot \left[\frac{F_{g,\gamma}(w, Q^2)}{VW}\left(\frac{1-v}{v} + \frac{v}{1-v}\right)\right.$$

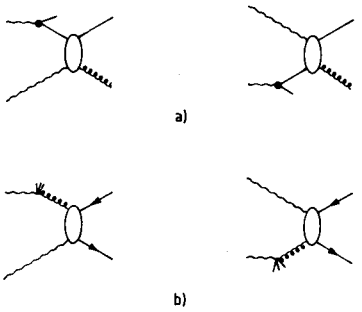

Fig. 3 a and b. Diagrams contributing to the leading logarithmic order: case where one of the photons interacts through its anomalous component. **a** The Compton like process $\gamma q \to gq$. **b** The fusion process $\gamma g \to q\bar{q}$

$$\left. + F_{g,\gamma}\left(\frac{1-v}{1-vw}Q^2\right)\cdot\left(\frac{1-v}{vw} + \frac{vw}{1-v}\right)\right]. \tag{29}$$

For our numerical study, we use the parametrization of Duke and Owens [4].

$$F_{q,\gamma}(x, Q^2) = \frac{\alpha}{2\pi} e_q^2 \ln\frac{Q^2}{\Lambda^2}\frac{1.81 - 1.67x + 2.16x^2}{1 - 0.4\ln(1-x)} x^{-0.3}$$

$$F_{g,\gamma}(x, Q^2) = \frac{\alpha}{2\pi}\ln\frac{Q^2}{\Lambda^2} 0.194(1-x)^{1.03} x^{-1.97},$$

$$\Lambda = 0.2\,\mathrm{GeV}. \tag{30}$$

Also contributing at the leading level are the terms where both photons scatter through their anomalous component (Fig. 4): such terms would appear explicitly in the calculation to second order in α_S. For completeness they are also included in our numerical calculation and the corresponding formulae are given in Appendix [27]. In general, these anomalous pieces, although of leading order, tend to be rather small at large p_T compared to the Born term because the initial energy is shared between a larger number of constituents. On the other hand, the "box" diagram [28] shown in Fig. 5 is of order α_S^2 but its contribution may be enhanced because of the two-body kinematics. It will also be included in our calculation.

In the next section we present a detailed discussion of the perturbative contributions (25)–(28) to the reaction $\gamma\gamma \to HX$ and delay to Sect. VI the presentation of the VDM estimates.

V. Numerical Results

Besides the anomalous photon component one needs to specify the fragmentation functions. The fragmentation of the quark and the gluon into pions is taken from Baier, Engels and Petersson [29]. Such a choice for quarks is in agreement with the data of PEP [30] and EMC [31] for $z > .5$: our predictions will therefore be reliable for values of p_T probing the large z region of the fragmentation function. We assume a suppression factor of 3.3 for a kaon compared to a pion when found

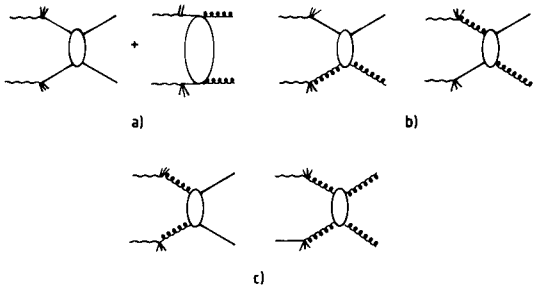

Fig. 4 a-c. Diagrams contributing to the leading logarithmic order; case where both photons interact through their anomalous components

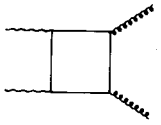

Fig. 5 The "box" diagram

in the fragments of a gluon or a non strange quark and the charged hadron spectrum is supposed to be dominated by the production of $\pi^{\pm}$ and $K^{\pm}$. Unless otherwise specified, all structure functions are defined in the non universal conventions described above. (This is necessary when only leading logarithmic parametrizations are available.) Because of phase space limitations, we consider the production of three flavors only, but the running coupling constant is calculated, in the leading logarithmic approximation, with four flavors. The value of Λ is 0.2 GeV. The results are presented for $\sqrt{s} = 8.5$ GeV a value representative of the PETRA energy range.

The Born cross-section (25) is presented in Fig. 6 for two "natural" choices of the factorization scale: $Q^2 = p_T^2$ and $Q^2 = S$. Both the $x_T (x_T = 2p_T/\sqrt{S})$ at rapidity zero and the rapidity dependence at $p_T = 3$ GeV/c are shown. The scaling violations in the quark fragmentation function reduce the spectrum for $x_T > 0.3$ when the larger factorization scale is used. It should be noted that the greater unstability in the prediction is obtained for the larger values of x_T where the perturbative calculation is expected to be most reliable: this points to the necessity of including higher order corrections. Under the same conventions, we show in Fig. 7 the anomalous piece normalized to the Born term: it rapidly decreases with increasing x_T, with more than 90% of the contribution at $x_T > .55$ due to the diagrams of Fig. 3a. The results are rather unstable with the choice of Q^2 specially at small x_T. Since, as mention in sect. III, the scale in the gluon fragmentation function is not well defined at the order at which the calculation is performed, we also present the results when the evolution of the gluon is frozen at $Q^2 = Q_0^2 = 25\,\text{GeV}^2$. The Q^2 dependence of the prediction in this case is much reduced. This illustrates the dominant rôle (at small x_T) played by (the scaling violations in) the fragmentation of the gluon. One can further remark

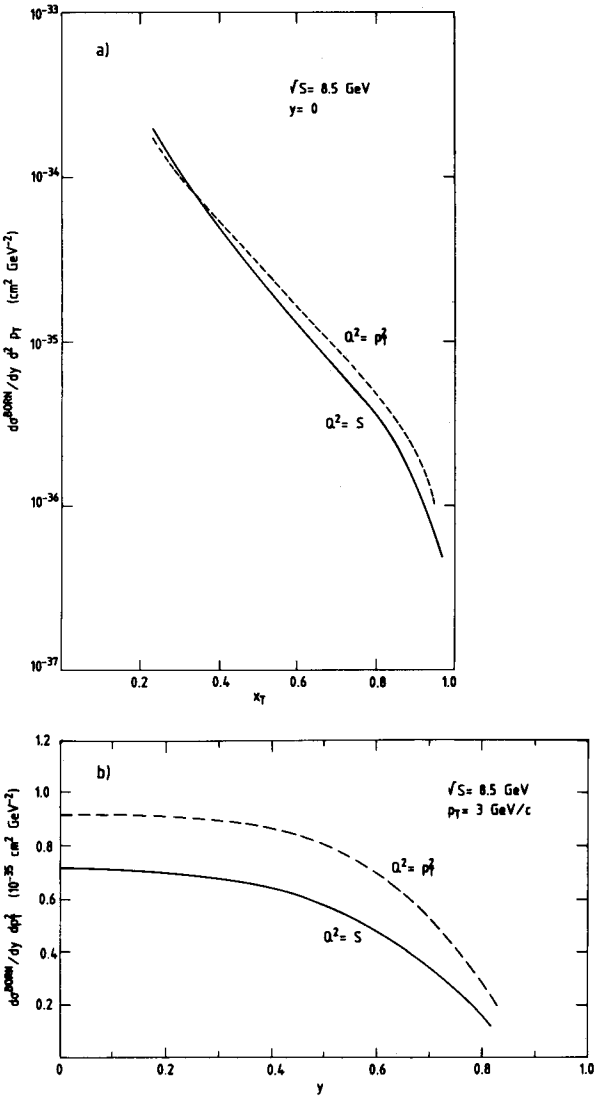

Fig. 6 a and b. The inclusive charged hadron differential cross-section at the Born level for the process $\gamma\gamma \to HX$, for two different factorization scales: $Q^2 = S$ (solid lines) and $Q^2 = p_T^2$ (dashed lines). **a** The dependence on x_T ($x_T = 2p_T/\sqrt{S}$) at 0 rapidity. **b** The rapidity dependence at $p_T = 3$ GeV/c

that increasing Q^2 enhances the photon anomalous component (proportional to $\ln Q^2/\Lambda^2$) while it softens the fragmentation functions. Both effects work in opposite direction in the single hadron spectrum but it can be seen that the latter wins over the former.

Figure 8 shows details on the behaviour of the corrections (28) normalized to the Born term. With the choice of scale $Q^2 = S$ the contribution of K_q is small, in agreement with [7] which related such a result to the absence of π^2 terms. Actually, terms proportional to terms $(1/(1-w))_+$ and $(\ln(1-w)/(1-w))_+$ are also lacking (see Appendix B). The dominance of the corrections by such factors was also noted in other processes [12, 13]. Most of the contribution to (28)

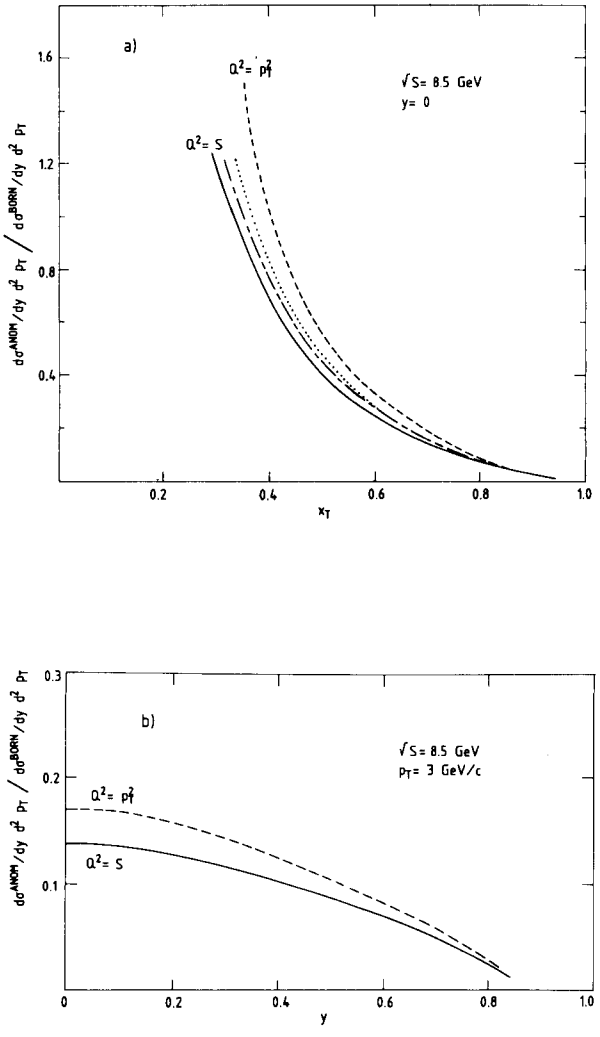

Fig. 7 a and b. The contribution of the anomalous terms to the inclusive charged spectrum normalised to the Born term for $\gamma\gamma \to HX$ for different factorization scales: $Q^2 = S$ (solid lines) and $Q^2 = p_T^2$ (dashed lines). **a** The x_T dependence; the dash dotted line (resp. the dotted line) shows the result for $Q^2 = S$ (resp. $Q^2 = p_T^2$) when the evolution of the gluon fragmentation function is frozen at $Q_0^2 = 25\,\mathrm{GeV}^2$. **b** The rapidity dependence

arises in fact from K_g but it is never large: at most 30% of the Born term in the relevant x_T range. A quite different pattern emerges when the scale $Q^2 = p_T^2$ is used (Fig. 8b). The contribution of K_g rapidly decreases from large and positive values at small x_T to rather large negative values for x_T near 1, whereas the previously negative K_g becomes positive but almost vanishes for $x_T > 0.6$. The variations in the structure of the corrections are easy to understand. From (12), (13) one sees that changing the scale from Q_1 to Q_2 introduces in the function K_g a piece of the form $(\alpha_s/2\pi)\ln(Q_1^2/Q_2^2)P_{qg}(1/\pi SZ)(d\hat{\sigma}^{\gamma\gamma\to q\bar{q}}/dv)$. The positivity of P_{qg} and $d\hat{\sigma}^{\gamma\gamma\to q\bar{q}}/dv$ implies then a larger correction when $Q_2 < Q_1$. A similar effect arises with the terms proportional to $P_{q\gamma}$ as is necessary to compensate for the decrease of the anomalous component when

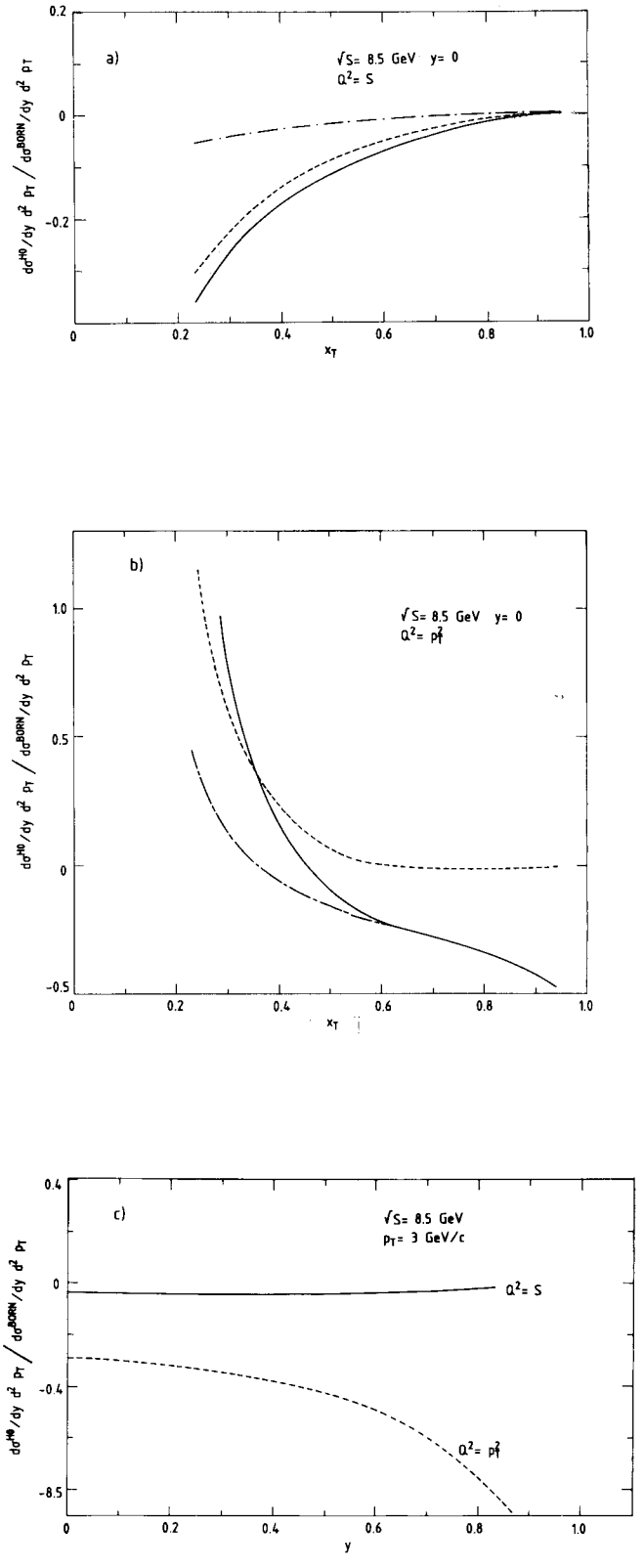

Fig. 8 a-c. The higher order corrections normalized to the Born cross-section for the process $\gamma\gamma \to HX$. **a** The contribution of K_q (dash dotted line), K_g (dotted line) and the total correction (solid line) for the choice of scale $Q^2 = S$; **b** The same as **a** with the scale $Q^2 = p_T^2$; **c** The rapidity dependence at $p_T = 3\,\mathrm{GeV/c}$

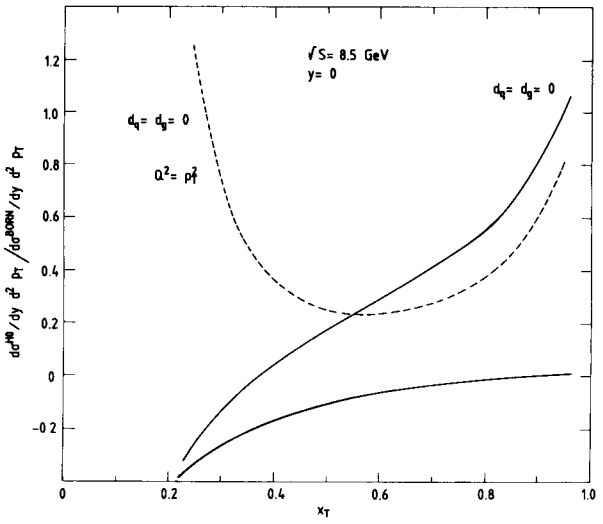

Fig. 9. The x_T dependence at $y = 0$, of the normalized higher order correction for various factorization prescriptions. The parameters f_q, d_q and d_g (see Appendix B for definitions) are all set equal to 1 unless otherwise specified. The solid curves refer to the scale $Q^2 = S$, the dashed one to $Q^2 = p_T^2$

$Q_2 < Q_1$. The case of K_q is slightly more complicated. The scale dependent term associated to P_{qq} is given by

$$\frac{\alpha_S}{2\pi}\ln\left(\frac{Q_1^2}{Q_2^2}\right)\frac{1}{\pi SZ}\frac{d\sigma^{\gamma\gamma\to q\bar{q}}}{dv}C_F$$

$$\left[2(\ln(1-Z)+\tfrac{3}{4})D_{q,H}(Z)\right.$$

$$\left.+\int_Z^1 dx\left(\frac{1+x^2}{x}D_{q,H}\left(\frac{Z}{x}\right)-2D_{q,H}(Z)\right)\Big/(1-x)\right] \quad (31)$$

after use is made of (14) and of the definition of $(1/(1-x))_+$. For Z values close to 1 (i.e. large x_T) the first term becomes large and negative (the second one is also negative but finite for usual choices of $D_{q,H}(x)$) implying an increase of the correction when the factorization scale increases. At small Z, the previous situation is recovered and the correction varies in the direction opposite to the change of scale. This behaviour is of course necessary to compensate for the changes occurring in the Born term (see Fig. 6a) and therefore to stabilize the fully corrected cross-section. We finally show in Fig. 8c the rapidity dependence of the normalized correction at $p_T = 3$ GeV/c. It is structureless and very small when $Q^2 = S$ but tends to become large and negative at the edge of phase space for the choice $Q^2 = p_T^2$: this illustrates again the important rôle played by the logarithmic term in (31). The dependence on the choice of the factorization prescription is studied in Fig. 9. The solid lines concern the results obtained with the scale $Q^2 = S$. One observes a drastic variation when going from the non-universal convention to the universal one ($d_g = d_q = 0$) in the quark fragmentation: for both choices of scales the behaviour of the correction at large x_T is affected showing a rapid growth with x_T. Of

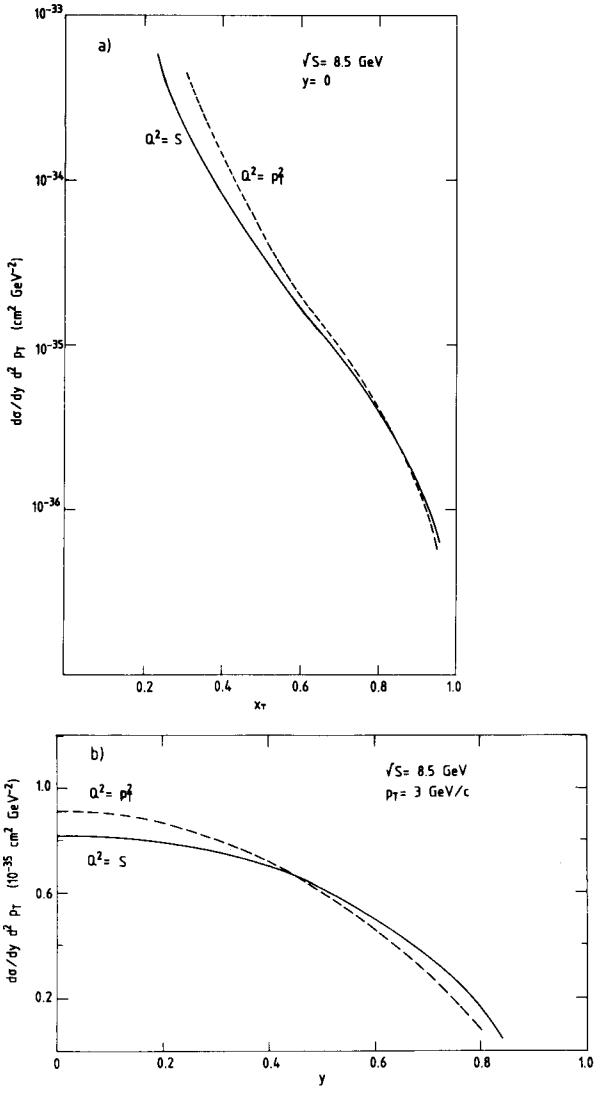

Fig. 10 a and b. The fully corrected charged hadron cross-section for the process $\gamma\gamma \to HX$. See Fig. 6 for the conventions

course, to each prescription corresponds a different shape of the fragmentation functions so that at order α_S the quantity $d\sigma^{\text{BORN}} + d\sigma^{\text{HO}}$ is independent on the choice of the factorization prescription. In Fig. 9 however, we have used for convenience the same fragmentation functions when comparing the ratio of the higher order corrections to the Born term in the universal and non-universal conventions since this ratio should not depend drastically on the shape of the fragmentation functions. The above discussion aims at emphasizing the dependence of the corrections on the scale and factorization prescription since in some works such aspects have been neglected [32] leading to essentially meaningless predictions. The $\gamma\gamma$ reaction because of its relative diagrammatic simplicity is quite pedagogical in this respect. Figure 10 shows the x_T and rapidity dependence of the full cross-section at $\sqrt{s} = 8.5$ GeV. We included in the cross-section the contri-

bution of the diagrams of Figs. 1 to 4 as well as the box diagram of Fig. 5 which however turns out to be small (at most 15% for $Q^2 = p_T^2$ at small x_T and much less otherwise). The main conclusion to be drawn from the comparison with Fig. 6 is an improvement in the stability of the prediction at the larger values of x_T. The lack of stability at small x_T is due partly to the inclusion of diagrams of Fig. 4, partly to the effects of scaling violations in the gluon fragmentation function which are not compensated at order $\alpha_S(\mu)$. In any case, the large x_T region where the VDM component is no longer dominant, as we shall see later, is the relevant region for confrontation with the data.

VI. Phenomenology of $e^+e^- \to e^+e^- HX$ with Untagged Leptons

We turn now to the estimate of the cross-section for the production of a single charged hadron in untagged e^+e^- collisions. We make the standard equivalent photon approximation which gives the flux of photons collinear to an electron or a positron as

$$P_{\gamma,e}(z) = \frac{\alpha}{\pi} \ln\left(\frac{P_e}{m_e}\right) \frac{(1+(1-z)^2)}{z} \tag{32}$$

where m_e and P_e are the mass and momentum of the charged lepton. We calculate then the rate for charged hadron production in untagged experiments by

$$E\frac{d^3\sigma}{d^3P} = \int dz_1 dz_2 P_{\gamma,e}(z_1) P_{\gamma,e}(z_2) E\frac{d^3\sigma^{\gamma\gamma\to HX}}{d^3P}\bigg|_{S=z_1z_2S_{ee}}. \tag{33}$$

The numerical evolution is performed with $P_e = 17\,\text{GeV/c}$ as in PETRA experiments. We plot in Fig. 11 what is designated as the K-factor i.e. the ratio of the fully corrected cross-section (25)–(29)* over the cross-section at the Born level (25). Several cases are considered. For the scale violating fragmentation functions used above, the results are given by the solid line ($Q^2 = S$) or the dashed line ($Q^2 = p_T^2$): the K-factor is small (1.22 to 1.30 at $p_T = 3\,\text{GeV/c}$) and decreasing with p_T due to the decrease of the anomalous component (the frozen gluon, not shown, gives very similar results). To further probe the rôle of the gluon, we display the results for a harder scale independent gluon fragmentation function of the form $(1-z)/z$ which has been found to give good agreement with the recent photoproduction data $\gamma p \to \pi^0 X$ at incident photon energy $\langle E_\gamma \rangle = 100\,\text{GeV}$ [33]. The K-factor is now slightly larger, in the range 1.4 to 1.5 at $p_T = 3\,\text{GeV/c}$ for the choices of scales $Q^2 = p_T^2$ and $Q^2 = S$ respectively. More important than the K-factor as a test of the validity of the perturbative calculation is the stability of the prediction under changes of scales: this is shown in Fig. 12 where the ratio of the differential cross-section calculated with $Q^2 = S$ to the differential cross-section with $Q^2 = p_T^2$ is plotted. The results are presented for our standard choices of fragmentation functions with or without scaling violations in the gluon fragmentation. In both cases the ratio is larger than 0.85 for $p_T \geqq 3\,\text{GeV/c}$ and increases to 1 for large p_T. (For the hard scaling gluon this ratio increases from 0.77 to 0.88 between 2 GeV/c and 5 GeV/c.) Also shown is the result for Born cross-sections for which this ratio is about 0.75 and nearly p_T independent.

The differential cross-section $d\sigma/dp_T$ is shown in Fig. 13 for the case $Q^2 = p_T^2$. Both the Born term and the fully corrected cross-section are displayed. The main purpose of this figure is to discuss the relevance of the perturbative calculation for inclusive hadron production in untagged e^+e^- experiments. We saw previously that the "error" on the perturbative result was $\pm 10\%$ or less for $p_T \geqq 3\,\text{GeV/c}$ for a large variation in the choice of the factorization scale. This gives an estimate on the internal consistency of the QCD result.

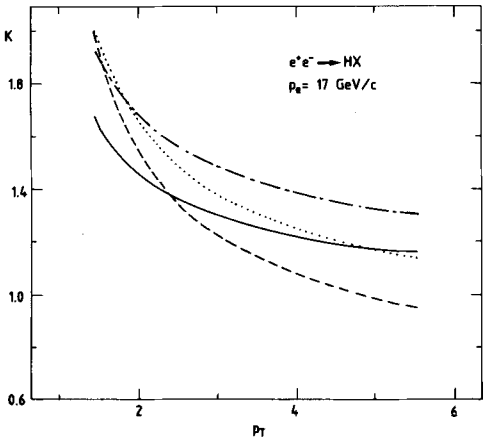

Fig. 11. The K-factor for the process $e^+e^- \to e^+e^- HX$ with untagged leptons at PETRA energies ($P_e = 17\,\text{GeV/c}$). The various curves correspond to the scale violating gluon fragmentation of [29], with the choice of factorization scale $Q^2 = S$ (solid line), $Q^2 = p_T^2$ (dashed line) and the hard scaling gluon $(1-z)/z$ with $Q^2 = S$ (dash dotted line) $Q_2 = p_T^2$ (dotted line)

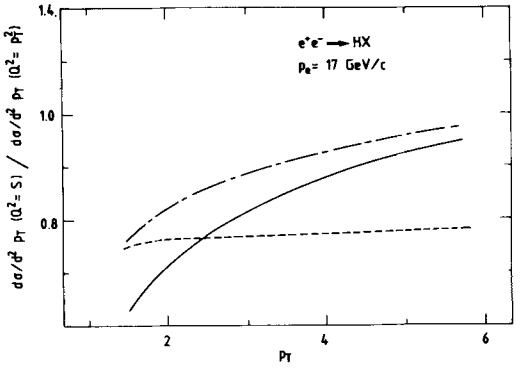

Fig. 12. Ratio of the differential cross-section $d\sigma/dp_T$ calculated with $Q^2 = S$ over the cross-section $Q^2 = p_T^2$ for the process $e^+e^- \to e^+e^- HX$: fully corrected cross-section with the gluon fragmentation of [29] (solid line) or the frozen gluon ($Q_0^2 = 25\,\text{GeV}$) (dash dotted line); Born cross-section (dashed line)

* Also included are the processes discussed in Appendix A, as well as the "box" diagram (Fig. 5)

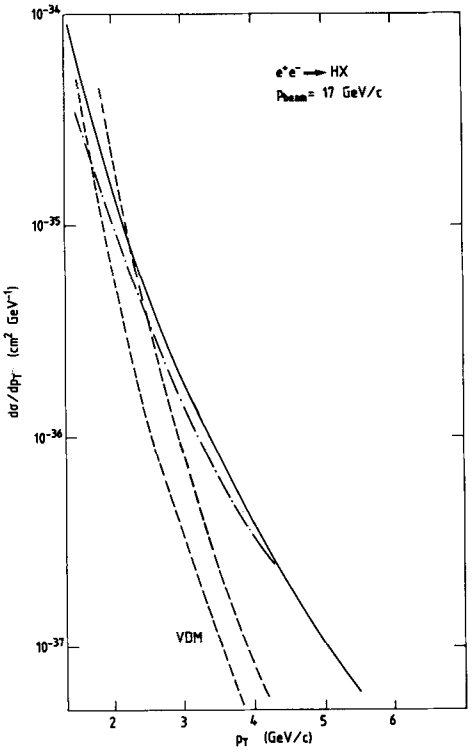

Fig. 13. The differential cross-section $d\sigma/dp_T$ for the process $e^+e^- \to e^+e^- HX$ for $p_{beam} = 17$ GeV/c. The Born term (dash dotted line), the fully corrected cross-section (solid line). The dashed lines represent the VDM contribution without intrinsic transverse momentum (lower curve) and including intrinsic transverse momentum (higher curve)

However, when comparing to the data one must also consider the contribution due to the hadronic component of the photon (VDM) as discussed in Sect. IV. The magnitude of the photon to resonance coupling can be obtained by comparing, for example, the photon–proton total cross-section to the pion–proton one [34] which yields the value $\sum_V(\alpha\pi/\gamma_V^2) \simeq 5\ 10^{-3}$. The parton distribution in the hadronic photon is then taken from the pion structure function. We use here the latest parametrization by Owens [35]. The VDM contribution is then calculated from the diagrams of Figs. 3 and 4 where at least one of the photons scatters through its VDM component. The result is given as the lower dashed line in Fig. 13: it rapidly decreases with p_T but it still gives a sizeable contribution up to $p_T = 2.5$ GeV/c. It is interesting to remark that the dominant contribution arises from the case where one of the photon couples perturbatively and the other one with its VDM structure function. A similar result is obtained (within 20%) if one takes for the photon VDM component the parametrization used in fits to the photon structure function, $F_2^{VDM}(x)/\alpha = 0.2(1-x)$ [36]. The above discussion leads in fact to a lower bound on the VDM contribution to the inclusive hadron spectrum. Indeed, it is well known that in hadron initiated reactions, the primordial parton transverse momentum considerably enhances the theoretical predictions at low p_T [37]. We therefore present a VDM estimate which includes such an effect. The method is to relate the VDM induced cross-sections directly to hadronic data in the way suggested in [1]. One writes

$$E\frac{d^3\sigma^{\gamma^{QCD}\gamma^{VDM}\to\pi^0X}}{d^3P} = \sum_V\left(\frac{\alpha\pi}{\gamma_V^2}\right)E\frac{d^3\sigma^{\gamma^{QCD}p\to\pi^0X}}{d^3P}\frac{2}{3}\frac{1}{(1-x_R)^2} \tag{34}$$

$$E\frac{d^3\sigma^{\gamma^{VDM}\gamma^{VDM}\to\pi^0X}}{d^3P} = \left(\sum_V\left(\frac{\alpha\pi}{\gamma_V^2}\right)\right)^2 E\frac{d^3\sigma^{pp\to\pi^0X}}{d^3P}\left(\frac{2}{3}\frac{1}{(1-x_R)^2}\right)^2 \tag{35}$$

where γ^{QCD} refers to the perturbative component of the photon and γ^{VDM} to its hadronic component. The factor $(2/3)1/(1-x_R)^2$ comes from the assumption of the dominance of qq scattering and gives the ratio of the meson form-factor over the nucleon form-factor including normalization and "dimensional counting". The variable x_R is the radial scaling variable $x_R = \sqrt{x_T^2 + x_L^2} = 2E/\sqrt{S}$. As input to (34) we use the result of our calculation of photoproduction reactions [12] which is in very good agreement with the NA14 data on $\gamma p \to \pi^0 X$ at 100 GeV [6], and for (35) we use the parametrization of Donaldson et al. [38] to their $pp \to \pi^0 X$ data at 100 GeV and 200 GeV with $p_T < 5$ GeV/c. The rate for the production of charged pions is then assumed to be twice that of π^0's and a ratio $K^\pm/\pi^\pm = 0.3$ is used. The relevant VDM contribution to untagged e^+e^- collisions is then obtained by convoluting the quantity

$$E\frac{d^3\sigma^{\gamma^{VDM}\gamma^{QCD}\to HX}}{d^3P} + E\frac{d^3\sigma^{\gamma^{QCD}\gamma^{VDM}\to HX}}{d^3P} + E\frac{d^3\sigma^{\gamma^{VDM}\gamma^{VDM}\to HX}}{d^3P}$$

with (32) as in (33). The result is shown by the upper dashed curve in Fig. 13. As expected, it falls above the theoretical estimates and still represents about 60% of the Born term at $p_T = 3$ GeV/c. It is noteworthy that the "theoretical" and "experimental" VDM estimates differ by a translation of roughly $\langle p_T \rangle = 0.35$ GeV/c over the whole p_T range shown: such a value is what is expected from intrinsic p_T effects and serves as a consistency check on our calculation of the VDM background.

The analysis above leads to results concerning the VDM contribution in deep contrast to that of Cello [10], and specially Tasso [9], which are essentially based on an exponentially falling distribution. We emphasize that, in our opinion, the hadronic component of the photon also undergoes hard scattering

leading to a power fall-off of the spectrum. Even more important at the larger p_T values is the contribution of the processes where one photon scatters through its VDM component and the other one through its perturbative component: the power fall-off in such a case is intermediate between the pure QCD generated spectrum and the double VDM one which represents less than 20% of the non-perturbative background for $p_T > 2\,\text{GeV/c}$.

Concerning the comparison to the data, if we ignore the effects of cuts on the experimentally measured quantities and apply our estimates we find that the VDM induced contribution and the corrections beyond the Born term more than double the naive estimates: we find a factor 2.6 at $p_T^2 = 6\,\text{GeV}^2/\text{c}^2$ and a factor 2 at $p_T^2 = 10\,\text{GeV}^2/\text{c}^2$. This is enough to put the Cello data in agreement with the theoretical estimates but is however too small to explain the Tasso data.

We show in Fig. 14 the results for LEP 1 with $P_e = 50\,\text{GeV/c}$. The differential cross-section at the Born level (dash dotted line) as well as the fully corrected perturbative cross-section (full line) are displayed with the choice of scale $Q^2 = p_T^2$. Concerning the VDM estimates two curves are given as before. The lower one corresponds to the "theoretical" estimate and is a straightforward extrapolation in energy of our calculation at $P_e = 17\,\text{GeV/c}$. The higher one takes into account the effect of primordial p_T in the following way: since there exists no photoproduction data at energies high enough to use (34) in the LEP energy range, we instead translate the "theoretical" curve by a primordial p_T value of 0.35 GeV/c as found at the lower energy. The figure shows that the VDM contribution is not negligible even at rather high p_T values: its contribution equals that of the Born term at $p_T \simeq 5\,\text{GeV/c}$. This is to be expected. Indeed at fixed p_T and for rising total energy, smaller and smaller x values of the hadronic photon are probed leading to a relative increase of the VDM contribution to the cross-section compared to the Born term.

In this paper, we calculate the contributions beyond the lowest order $\gamma\gamma \to q\bar{q}$ diagrams to the single hadron spectrum in untagged e^+e^- experiments. We give the complete analytic expressions of the perturbative corrections and find that they are large at low x_T values at both PEP/PETRA and LEP energies: this is due to the pieces which contain the anomalous photon component. The non perturbative contributions are estimated

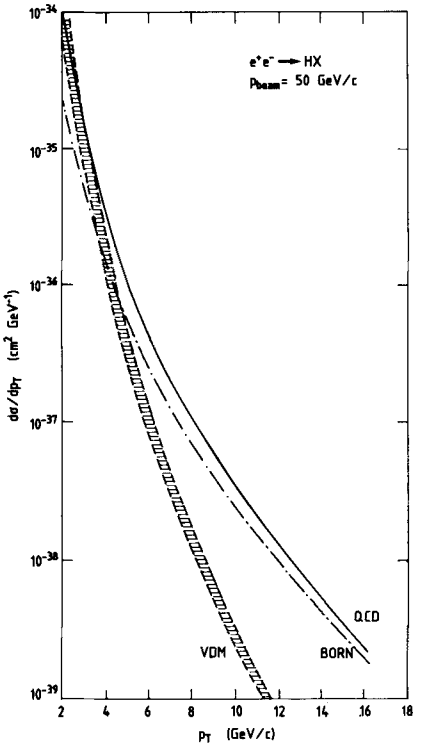

Fig. 14. Same as Fig. 13 at $p_{\text{beam}} = 50\,\text{GeV/c}$

using the vector dominance model of the photon and they are found to be important up to rather large values of p_T: typically they are equal to the Born term for $p_T = 2.8\,\text{GeV/c}$ at PETRA and $p_T = 5\,\text{GeV/c}$ at LEP. However, they have a faster fall-off in p_T than the perturbative contributions. An unambiguous test of the QCD predictions would therefore require collecting data at large enough values of p_T where the VDM contribution becomes negligible.

Appendix A

We list below the contributions to the single inclusive cross-section of configurations where each initial photon scatters through its hadronic constituents. All flavors are assumed to be massless and $F_{q\gamma} = F_{\bar{q}\gamma}$

Fig. 4a:

$$E\frac{d^3\sigma}{d^3P} = \frac{C_F N_C}{S p_T^2} \sum_{i=q,\bar{q}} \int_{1-V+VW}^{1} dx \int_{VW/x}^{1-(1-V)/x} dv F_{i,\gamma}\left(\frac{VW}{vx}, Q^2\right) F_{i,\gamma}\left(\frac{1-V}{(1-v)x}, Q^2\right) \alpha_S^2(Q^2)$$
$$\left\{2\left[C_F\left(\frac{v}{1-v} + \frac{1-v}{v}\right) - N_C(v^2 + (1-v)^2)\right] D_{g,H}(x, Q^2)\right.$$
$$+ \left[\frac{1+v^2}{(1-v)^2} + v^2 + (1-v)^2 + 2\frac{1+(1-v)^2}{v^2} + \frac{2}{N_C}\left(\frac{(1-v)^2}{v} - \frac{1}{v(1-v)}\right)\right] \bar{D}_{i,H}(x, Q^2)$$
$$\left. + \left[\frac{1+v^2}{(1-v)^2} + v^2 + (1-v)^2 + \frac{2}{N_C}\frac{v^2}{1-v}\right] \bar{D}_{i,H}(x, Q^2) + [v^2 + (1-v)^2] \sum_{j \neq i,\bar{i}} \bar{D}_{j,H}(x, Q^2)\right\}$$

$$+\frac{C_F N_C}{S p_T^2}\sum_{i=q,\bar{q}}\sum_{j=q,\bar{q}}\int_{1-V+VW}^{1}dx\int_{VW/x}^{1-(1-V)/x}dv F_{j,\gamma}\left(\frac{VW}{vx},Q^2\right)F_{i,\gamma}\left(\frac{1-V}{(1-v)x},Q^2\right)\alpha_S^2(Q^2)$$
$$\cdot\left\{\frac{1+(1-v)^2}{v^2}\bar{D}_{i,H}(x,Q^2)+\frac{1+v^2}{(1-v)^2}\bar{D}_{j,H}(x,Q^2)\right\}$$

Fig. 4b:

$$E\frac{d^3\sigma}{d^3P}=\frac{2C_F N_C}{S p_T^2}\int_{1-V+VW}^{1}dx\int_{VW/x}^{1-(1-V)/x}dv\alpha_S^2(Q^2)\sum_{i=q,\bar{q}}\left\{F_{g,\gamma}\left(\frac{VW}{vx},Q^2\right)F_{i,\gamma}\left(\frac{1-V}{(1-v)x},Q^2\right)\right.$$
$$\cdot\left[\left(C_F\left(\frac{1}{v}+v\right)+N_C\frac{1+v^2}{(1-v)^2}\right)D_{g,H}(x,Q^2)+\left(C_F\left(\frac{1}{1-v}+1-v\right)+N_C\frac{1+(1-v)^2}{v^2}\right)\bar{D}_{i,H}(x,Q^2)\right]$$
$$+F_{i,\gamma}\left(\frac{VW}{vx},Q^2\right)F_{g,\gamma}\left(\frac{1-V}{(1-v)x},Q^2\right)\left[\left(C_F\left(\frac{1}{1-v}+(1-v)\right)+N_C\frac{1+(1-v)^2}{v^2}\right)D_{g,H}(x,Q^2)\right.$$
$$\left.\left.+\left(C_F\left(\frac{1}{v}+v\right)+N_C\frac{1+v^2}{(1-v)^2}\right)\bar{D}_{i,H}(x,Q^2)\right]\right\}$$

Fig. 4c:

$$E\frac{d^3\sigma}{d^3P}=\frac{2C_F N_C}{S p_T^2}\int_{1-V+VW}^{1}dx\int_{VW/x}^{1-(1-V)/x}dv\alpha_S^2(Q^2)F_{g,\gamma}\left(\frac{VW}{vx},Q^2\right)F_{g,\gamma}\left(\frac{1-V}{(1-v)x},Q^2\right)$$
$$\cdot\left\{\left(C_F\left(\frac{v}{1-v}+\frac{1-v}{v}\right)-N_C(v^2+(1-v)^2)\right)\sum_{i=q,\bar{q}}\bar{D}_{i,H}(x,Q^2)\right.$$
$$\left.+4N_C^2\left(3-v(1-v)+\frac{v}{(1-v)^2}+\frac{1-v}{v^2}\right)D_{g,H}(x,Q^2)\right\}.$$

Appendix B

The higher order corrections $K_q(v,w,Q^2,S)$ and $K_g(v,w,Q^2,S)$ of (28) can be written in the following form [17]

$$K_q(v,w,Q^2,S)$$
$$=\alpha^2 e_q^4\frac{2C_F N_C}{S p_T^2}x^2\left\{c_1\delta(1-w)+c_2\left(\frac{1}{1-w}\right)_+\right.$$
$$+c_3\left(\frac{\ln(1-w)}{1-w}\right)_+ +\left(cD_4\delta(1-w)+cW_4\right.$$
$$\left.\cdot\left(\frac{1}{1-w}\right)_+ +c_4\right)\ln\left(\frac{S}{Q^2}\right)$$
$$+c_5\ln v+c_6\ln(1-vw)+c_7\ln(1-v+vw)$$
$$+c_8\ln(1-v)+c_9\ln w+c_{10}\ln(1-w)+c_{11}$$
$$+c_{12}\frac{\ln(1-v+vw)}{1-w}$$
$$\left.+c_{13}\frac{\ln w}{1-w}+c_{14}\frac{\ln((1-vw)/(1-v))}{1-w}\right\}$$

and similarly for $K_g(v,w,Q^2,S)$ with coefficients c_i'. The variables v,w are defined in (6). The coefficients listed below depend on the parameters f_q, d_q and d_g. The parameter f_q is set equal to 1 for the non universal definition of the photon structure function (see (23), (24)) and it vanishes for the universal convention. Likewise $d_q=d_g=1$ if (21) are used and $d_q=d_g=0$ for the universal definition of the quark fragmentation function. In the expressions below one uses the notation

$$x_1=1-vw$$
$$x_2=1-v+vw.$$
$$c_1=\left(1-v-\frac{1}{2v}\right)\left(7-\frac{4\pi^2}{3}\right)-\left(1+2v-\frac{3}{2v}\right)\ln v$$
$$+\left(-2+3v+\frac{2}{v}\right)\ln^2 v+(2+v)\ln(1-v)$$
$$+\left(-2+v+\frac{2}{v}\right)\ln^2(1-v)+d_q\left(1-v-\frac{1}{2v}\right)$$
$$\cdot\left(\frac{4\pi^2}{3}-9-3\ln v+2\ln^2 v\right)$$
$$c_2=\left(1-v-\frac{1}{2v}\right)(3-4\ln v)(1-d_q)$$
$$c_3=-4\left(1-v-\frac{1}{2v}\right)(1-d_q)$$
$$cD_4=-\left(1-v-\frac{1}{2v}\right)(3+4\ln v)$$

$$cW_4 = -4\left(1-v-\frac{1}{2v}\right)$$

$$c_4 = -6+6v-4v^2+\frac{1}{v}+f(v,w)+h(v,w)+2\frac{(1-v)^2}{x_2}$$

$$c_5 = c_4+f_q(3-4v+2v^2+v(1-2v)w+v^2w^2-h(v,w))+d_q\left(g(v,w)-2\frac{(1-v)^2}{x_2}\right)$$

$$c_6 = 2(3-2v+2v^2-2v^2w+v^2w^2)$$

$$c_7 = 2\left(1+2\frac{(1-v)^2}{x_2}+d_q\left(g(v,w)-2\frac{(1-v)^2}{x_2}\right)\right)$$

$$c_8 = -2(1+(1-v)^2)-f_q(3-4v+2v^2+v(1-2v)w+v^2w^2-h(v,w))$$

$$c_9 = -2(1+v+vw+v^2w^2)+f_q\left(-1+v-v^2+\frac{1}{v}\right)(w^2+(1-w)^2)$$

$$c_{10} = -8+6v-6v^2+\frac{1}{v}+4v^2w-2v^2w^2+f(v,w)+h(v,w)+2\frac{(1-v)^2}{x_2}+f_q\left(6-6v+4v^2-\frac{1}{v}-f(v,w)-g(v,w)-h(v,w)\right)+d_q\left(g(v,w)-2\frac{(1-v)^2}{x_2}\right)$$

$$c_{11} = -\tfrac{9}{2}+2v-2v^2+\frac{3}{v}+\left(-6+3v+\frac{5}{v}\right)w+\left(6-v-2v^2-\frac{6}{v}\right)w^2-6\frac{(1-v)^2}{x_1^3}+\frac{11-17v+6v^2}{x_1^2}+\frac{-4+8v-v^2}{x_1}-2\frac{(1-v)^2}{x_2}+3f_q\left(-2(1-v)^2+2v^2w^2-\frac{1}{x_1}+f(v,w)+h(v,w)\right)+\tfrac{3}{2}d_q(1-3v+v^2-vw+v^2w^2)$$

$$c_{12} = -4\left(1-v+\frac{1}{2v}\right)+8d_q\left(1-v-\frac{1}{2v}\right)$$

$$c_{13} = 2\left(v+\frac{1}{v}\right)$$

$$c_{14} = 2\left(2-v-\frac{2}{v}\right)$$

with the definitions

$$f(v,w) = 2\left(v^2+(1-v)^2-\frac{1}{v}\right)w+2\left(-1+v-2v^2+\frac{1}{v}\right)w^2$$

$$g(v,w) = 2-v+v^2+vw+v^2w^2$$

$$h(v,w) = 2\frac{(1-v)^2}{x_1^3}-2\frac{(1-v)(2-v)}{x_1^2}+\frac{5-6v+2v^2}{x_1}$$

$$c'_4 = 8(2(1-v)+(1-v+v^2)(1-w+w^2)+p(v,x_1)+p(v,x_2))$$

$$c'_5 = 8\left((1-v+v^2)(1-w+w^2)+(1-v)^2\left(\frac{1}{x_1}\left(\frac{1}{x_1}-\frac{2}{2-v}\right)+\frac{1}{x_2}\left(\frac{1}{x_2}-\frac{2}{2-v}\right)\right)\right)+2f_q(q(v,w)-4p(v,x_1))+2d_g(r(v,w)-4p(v,x_2))$$

$$c'_6 = 4(4(1-v)+q(v,w))$$

$$c'_7 = 16(1-v+p(v,x_2))+4d_g(r(v,w)-4p(v,x_2))$$

$$c'_8 = 4\left(-3+v^2+\frac{4}{v}-2vw+2vw^2+2\left(1-v-\frac{1}{v}+\frac{1}{2-v}\right)\cdot\left(\frac{1}{x_1}+\frac{1}{x_2}\right)\right)-2f_q(q(v,w)-4p(v,x_1))$$

$$c'_9 = 4(-2(1-v)+2(1-v)w+v^2w^2+\frac{2}{x_1}\left(3-2v+v^2-\frac{1}{v}-\frac{1}{2-v}\right)+\frac{2}{x_2}\left(-1+v+\frac{1}{v}-\frac{1}{2-v}\right))+2f_q(1+(1-v)^2)(w^2+(1-w)^2)$$

$$c'_{10} = 4(3(1+(1-v)^2)+4(-1+v-v^2)w+(2-2v+3v^2)w^2+\frac{2}{x_1}\left(-3+4v-v^2+\frac{1}{v}-\frac{1}{2-v}\right)+\frac{2}{x_2}\left(1+v-\frac{1}{v}-\frac{1}{2-v}\right)+2(1-v)^2\left(\frac{1}{x_1^2}+\frac{1}{x_2^2}\right))+2f_q(-(1+(1-v)^2)(w^2+(1-w)^2)+q(v,w)-4p(v,x_1))+2d_g(r(v,w)-4p(v,x_2))$$

$$c'_{11} = 4(1+(1-v)^2+v^2w^2)+4d_g(2-v-vw+2p(v,x_2))$$

$$+ 12 f_q(2 - 3v + v^2 + (-2 + 3v - 2v^2)w + (2 - 2v + v^2)w^2 + 2p(v, x_1))$$

with

$$p(v,x) = \frac{1-v}{x}\left(\frac{1-v}{x} - 2 + v\right)$$

$$q(v,w) = -5 + 6v - 2v^2 - 2v(1-v)w - v^2w^2$$

$$r(v,w) = -5 + 4v - v^2 + 2vw - v^2w^2.$$

References

1. S.J. Brodsky, T.A. De Grand, J.F. Gunion, J.H. Weis: Phys. Rev. Lett. **41**, 672 (1978); Phys. Rev. **D19**, 1418 (1979)
2. T. Jayaraman: Contribution to the VIth International Workshop on Photon–Photon Collisions (Lake Tahoe, Calif., 10–13 Sept. 1984)
3. J.C. Pati, A. Salam: Phys. Rev. Lett. **36**, 11 (1976); A.V. Efremov, S.V. Ivanov: Dubna preprint E2-81–285; A. Janah, M. Ozer: Univ. of Maryland preprint 81–221; T. Jayaraman, G. Rajasekaran, S.D. Rindani: Phys. Lett. **119B**, 215 (1982); R.M. Godbole et al.: Phys. Lett. **142B**, 91 (1984)
4. D.W. Duke, J.F. Owens: Phys. Rev. **D26**, 1600 (1982); Erratum Phys. Rev. **D28**, 1227 (1983)
5. P. Aurenche, et al.: Z. Phys. C—Particles and Fields **24**, 309 (1984)
6. NA14 Collab. P. Astbury et al.: CERN/EP/85.07; Ian Siotis, talk presented at the XVth Symposium on Multiparticle Dynamics, Lund 1984
7. F. Khalafi, P.V. Landshoff, W.J. Stirling: Phys. Lett. **130B**, 215 (1983)
8. F. Khalafi: U. College London, March 1984
9. TASSO Collab. M. Althoff et al.: Phys. Lett. **138B**, 219 (1984)
10. CELLO Collaboration: Contribution to the XXII International Conference on High Energy Physics, Leipzig, 1984
11. Several good reviews on photon–photon physics exist: J.B. Dainton: Rutherford Laboratory preprint RL. 83–103; H.-J. Behrend: Talk presented at the Symposium on High Energy e^+e^- Interactions at Vanderbilt University, April 1984; H. Kolanoski: Summary Talk on the two-photon session, XXII International Conf. on High Energy Physics, Leipzig, 1984
12. P. Aurenche et al.: Phys. Lett. **135B**, 164 (1984)
13. P. Aurenche et al.: Phys. Lett. **140B**, 87 (1984)
14. F.A. Berends, Z. Kunszt, R. Gastmans: Nucl. Phys. **B182**, 397 (1981); I. Kang, Oxford University preprint 50/82
15. G. 't Hooft, M. Veltman: Nucl. Phys. **B144**, 189 (1972); C.G. Bollini, J.J. Giambiagi: Nuovo Cimento **12B**, 20 (1972); W.J. Marciano: Phys. Rev. **D12**, 3861 (1975)
16. H.D. Politzer: Nucl. Phys. **B129**, 301 (1977); D. Amati, R. Petronzio, G. Veneziano: Nucl. Phys. **B146**, 29 (1978); A.H. Mueller: Phys. Rev. **D18**, 3705 (1978); S.B. Libby, G. Sterman: Phys. Rev. **D18**, 3257 (1978); R.K. Ellis et al.: Nucl. Phys. **B152**, 285 (1979)
17. R.K. Ellis, M.A. Furman, H.E. Haber, I. Hinchliffe: Nucl. Phys. **B173**, 397 (1980)
18. P. Aurenche, J. Lindfors: Nucl. Phys. **B168**, 296 (1980)
19. A. Douiri: Thèse de Doctorat d'Etat, Grenoble (1984)
20 M.A. Nowak, M. Praszałowicz, W. Słonimski: Max-Planck Institute preprint MPI/PTH 14/84
21. R. Baier, K. Fey: Z. Phys. C—Particles and Fields **2**, 339 (1979)
22. G. Altarelli, R.K. Ellis, G. Martinelli, So-Young Pi: Nucl. Phys. **B160**, 301 (1979)
23. R.L. Kingsley: Nucl. Phys. **B60**, 45 (1973); T.F. Walsh, P. Zerwas: Phys. Lett. **44B**, 195 (1973); M.A. Ahmed, G.C. Ross: Phys. Lett. **59B**, 369 (1975)
24. This equation is easily derived from the expression of $f_{qg}(x)$ calculated in G. Alterelli, R.K. Ellis, G. Martinelli: Nucl. Phys. **B143**, 521 (1978); Erratum **B147**, 544 (1978)
25. E. Witten: Nucl. Phys. **B120**, 189 (1977); C.H. Llewellyn-Smith, Phys. Lett. **79B**, 83 (1978); R.J. de Witt et al.: Phys. Rev. **D19**, 2046 (1979); Erratum Phys. Rev. **D20**, 1751 (1979); W. Frazer, J. Gunion: Phys. Rev. **D20**, 147 (1979)
26. M. Glück, E. Reya: Phys. Rev. **D28**, 2749 (1983)
27. See also K. Kajantie: Acta Phys. Austr. Suppl. XXI, 663 (1979)
28. K. Kajantie, R. Raitio: Phys. Lett. **87B**, 133 (1979); R.N. Cahn, J.F. Gunion: Phys. Rev. **D20**, 2253 (1979)
29. R. Baier, J. Engels, B. Petersson: Z. Phys. C—Particles and Fields **2**, 265 (1979)
30. Mark II Collab. J.F. Patrick et al.: Phys. Rev. Lett. **49**, 1232 (1982)
31. EMC Collab. R. Windmolders: Talk presented at the XI International Symposium on Multiparticle Dynamics, Lund 1984
32. A.P. Contogouris, H. Tanaka: McGill University preprint, "K-factor for processes involving real photons", May 1984
33. G. Wormser: Thèse de Doctorat d'Etat, Orsay (1984)
34. For a compilation of the data, see Reviews of Particle Properties. Rev. Mod. Phys. **56** (1984); See also [6]
35. J.F. Owens: Phys. Rev. **D30**, 943 (1984)
36. I.F. Ginzburg, V.G. Serbo: Phys. Lett. **109B**, 231 (1982); See also J.B. Daiton: [11]
37. R. Baier, J. Engels, B. Petersson: Z. Phys. C—Particles and Fields **6**, 309 (1980)
38. G. Donaldson et al.: Phys. Lett. **73B**, 375 (1978)